ISSN 0554-6397
UDK: 004.032.26
Original scientific paper
Received: 8th March 2022.

Vedran Mrzljak
E-mail: vedran.mrzljak@riteh.hr
Tomislav Senčić
E-mail: tomislav.sencic@riteh.hr
Faculty of Engineering, University of Rijeka, Vukovarska 58, 51000 Rijeka, Croatia
Igor Poljak
E-mail: ipoljak1@unizd.hr
Department of Maritime Sciences, University of Zadar, Mihovila Pavlinovića 1, 23000 Zadar, Croatia
Vedran Medica-Viola
Faculty of Engineering, University of Rijeka, Vukovarska 58, 51000 Rijeka, Croatia
E-mail: vmedica@riteh.hr

Thermodynamic Analysis of Steam Cooling Process in Marine Power Plant by Using Desuperheater

Abstract

Thermodynamic (energy and exergy) analysis of steam cooling process in the marine steam propulsion plant is presented in this research. Steam cooling is performed by using Desuperheater which inject water in the superheated steam to obtain wet steam. Wet steam is used in auxiliary heaters for various heating purposes inside the marine steam propulsion system. Auxiliary heaters require wet steam due to safety reasons and for easier steam condensation after heat transfer. Analysis of steam cooling process is performed for a variety of steam system loads. Mass flow rates of cooling water and superheated steam in a properly balanced cooling process should have the same trends at different system loads - deviations from this conclusion is expected only for a notable change in any fluid temperature. Reduction in steam temperature is dependable on the superheated steam temperature (at Desuperheater inlet) because the temperature of wet steam (at Desuperheater outlet) is intended to be almost constant at all steam system loads. Energy losses of steam cooling process for all observed system loads are low and in range between 10–30 kW, while exergy losses are lower in comparison to energy losses (between 5–15 kW) for all loads except three the highest ones. At the highest system loads exergy losses strongly increase and are higher than 20 kW (up to 40 kW). The energy efficiency of a steam cooling process is very high (around 99% or higher), while exergy efficiency is slightly lower than energy efficiency (around 98% or higher) for all loads except the highest ones. At the highest steam system loads, due to a notable increase in cooling water mass flow rate and high temperature reduction, steam cooling process exergy efficiency significantly decreases, but still remains acceptably high (between 95% and 97%). Observation of both energy and exergy losses and efficiencies leads to conclusion that exergy analysis consider notable increase in mass flow rate of cooling water which thermodynamic properties (especially specific exergies) strongly differs in comparison to steam. Such element cannot be seen in the energy analysis of the same system.

Keywords: Steam cooling, Desuperheater, Thermodynamic analysis, Marine power plant

1. Introduction

Marine propulsion systems are nowadays dominantly based on the internal combustion engines. There are numerous variations related to marine diesel engines which can be used for propulsion purposes such as: four-stroke fast or middle speed diesel engines [1, 2], two-stroke low speed diesel engines [3, 4] and in a recent time dual fuel engines [5-7] which show many benefits in comparison to standard diesel engines. The dominancy of internal combustion engines in marine propulsion systems leads to the development of various techniques for their processes improving as well as emissions reduction [8-10].

Along with diesel and dual fuel internal combustion engines, for marine propulsion purposes can be used various other mechanical power producers such as gas and steam turbines [11-13]. At the moment, it is also not a rarity to find complex marine propulsion systems in which are incorporated two or more mechanical power producers [14-16].

Steam propulsion systems are still important in the propulsion of various LNG carriers, but its domination in the past is significantly diminished at the moment by dual fuel internal combustion engines implementation [17, 18]. It can be expected that in the near future, dual fuel internal combustion engines will take precedence also in the propulsion of LNG carriers.

Due to the specificity of its operation, marine steam propulsion systems have various specific elements and subsystems in comparison to conventional land-based steam power plants [19, 20]. One of such specific process, which is usually not required in the land-based steam power plant is steam cooling process. In the most of the cases, the steam cooling process in the marine steam propulsion system is performed by using a device called Desuperheater [21, 22]. Superheated steam is cooled by water injection (direct mixing of water and superheated steam), where Desuperheater regulates water mass flow rate. The intention of steam cooling process in marine propulsion system is a wet steam production which will be used in marine auxiliary heaters.

In this paper will be performed thermodynamic (energy and exergy) analysis of steam cooling process by using Desuperheater in the marine steam propulsion plant which operates at the commercial LNG carrier. The analysis will be performed at various power plant (steam system) loads by using measured data from exploitation with an aim to investigate the effectiveness of this process in different operating regimes. Especially important will be to analyze how the change in cooling water mass flow rate influences efficiencies and losses of steam cooling process and what are the main tasks of Desuperheater regulating system to ensure proper operation in any power plant operating regime.

2. Description and characteristics of steam cooling process by using Desuperheater

The steam cooling process by using Desuperheater is just one of many complex processes in the marine steam power plant. Marine steam propulsion power plant in which operates analyzed Desuperheater and for which will be analyzed steam cooling process operates at the 84812 DWT commercial LNG carrier, which overall length is 288 m and maximum breadth equals 44 m.

A simplified scheme of the LNG carrier steam propulsion power plant is presented in Figure 1, along with Desuperheater position and all inlet and outlet fluid streams required for the steam cooling process analysis. Propulsion plant consist of two identical marine steam generators Mitsubishi MB-4E-KS [23, 24] which produces superheated steam (main steam) for all steam turbines in the plant as well as auxiliary steam (steam with lower temperature in comparison to main steam) for ship auxiliary requirements [25]. Main steam is delivered to two turbo-generators (TG1 and TG2), to main propulsion turbine and to low-power steam turbine with one Curtis stage for the main feedwater pump drive. Each turbo-generator has maximum power of 3850 kW, while low-power steam turbine for the main feedwater pump drive has maximum power of 570 kW [26]. Main propulsion steam turbine consists of two cylinders: Low Pressure Cylinder (LPC) and High Pressure Cylinder (HPC). Between main turbine cylinders steam re-heating process did not occur, while maximum power of the entire main turbine (both cylinders) equals 29420 kW [27]. Main turbine is used for the propulsion propeller drive, as presented in Figure 1.

Steam after expansion in both turbo-generators and in both main turbine cylinders is delivered to the main condenser for condensation, while steam after expansion in low-power steam turbine for the main feedwater pump drive is delivered to the deaerator. Obtained condensate in main condenser is delivered by a condensate pump to deaerator (before deaerator occurs condensate heating process in the low pressure condensate heater) [28]. After additional heating and deaerating in the deaerator, feedwater is taken by the main feedwater pump and delivered to both steam generators. Before steam generators, feedwater is additionally heated in the high pressure feedwater heater [29]. Another important component is hot well, which collects all the condensate from the power plant and deliver it by the auxiliary pump to the main condensate line [30].

As can be observed from Figure 1, Desuperheater is mounted after the main feedwater pump and before the high pressure feedwater heater. Cooling water which will be injected in superheated steam is taken from the feedwater branch and after pressure reduction (by using pressure reducing valve) is delivered to Desuperheater. The Desuperheater regulation process is pneumatic, therefore air compressed by marine compressors must also be delivered to Desuperheater. Before delivering to Desuperheater inlet, auxiliary steam produced in steam generators also passes through a pressure reducing valve which decreases its pressure, but in any plant operating regime steam at the Desuperheater inlet is superheated. Cooling water is injected into

the superheated steam which temperature decreases and produced wet steam (at the Desuperheater outlet) is delivered to auxiliary heaters. There are several auxiliary heaters in this marine steam power plant: service heater, fuel heater, LNG vapor heater and water heater. However, in similar marine steam power plants can also be found other auxiliary heaters (along with described four).

The main reason of applying superheated steam cooling process before auxiliary heaters is to protect heat exchange pipes of each auxiliary heater. Materials used in each auxiliary heat exchanger are not capable to withstand superheated steam parameters, especially not for a long time, therefore superheated steam cooling process is necessary for proper operation of each auxiliary heater. Another reason for superheated steam cooling before auxiliary heaters is that after the heat exchange in each auxiliary heater, wet steam condenses and obtained condensate is delivered to the hot well. If the superheated steam is used for auxiliary heaters operation, there is no guarantee that it will condense at the outlet of each auxiliary heater, so in hot well will be delivered a notable amount of steam which would cause many problems (and possible hot well breakdown).

Finally, it can be concluded that the superheated steam cooling process is necessary for producing proper fluid (wet steam) for long, safe and reliable operation of all auxiliary heaters.

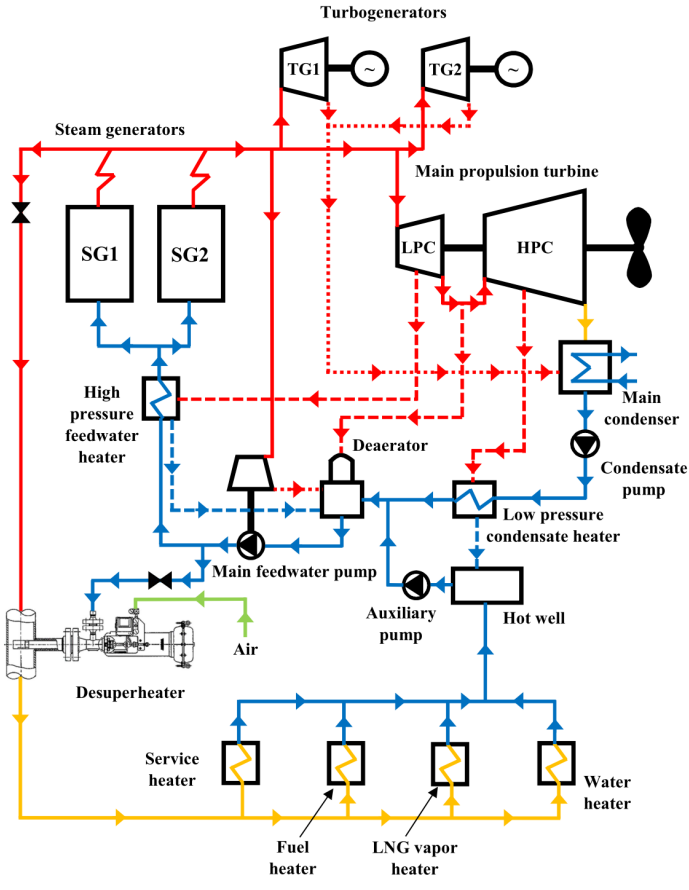

Figure 1 - Desuperheater position in marine steam propulsion power plant and the principle of steam cooling process (blue = water/condensate; red = superheated steam; orange = wet steam; green = air)

Closer look of Desuperheater along with all the fluids required for its operation is presented in Figure 2. Air required for Desuperheater regulation is delivered to the upper part and the lowest required air pressure is 4 bar [31]. Such air pressure is not problematic, it can easily be delivered from marine compressors which increases air pressure not only for Desuperheater regulation, but also for other marine devices.

Through middle Desuperheater part passes cooling water through independent connection. Cooling water circulates from the middle to the lower Desuperheater part which will be presented more detail in the next figure (DETAIL 1) where is injected into the superheated steam stream (steam inlet). As can be seen from Figure 2,

cooling water is injected in the same flow direction as superheated steam. After water injection and after proper mixing with superheated steam (ensured by nozzles at the Desuperheater bottom) from superheated steam is obtained wet steam with notably decreased temperature and slightly decreased pressure (steam outlet). As mentioned before, obtained wet steam will be delivered to auxiliary heaters.

For the proper thermodynamic (energy and exergy) analysis of the superheated steam cooling process are required operating parameters measured in all three operating points presented in Figure 2 (operating point A for superheated steam, operating point B for cooling water and operating point C for wet steam). In each operating point, at each steam system load, measurements of each fluid temperature, pressure and mass flow rate are required.

Calculations will be performed according to recommendations from the literature by using principles of open heat exchangers (in which occur operating fluids mixing) – the same mixing of operating fluids (cooling water and superheated steam) occurs in the observed steam cooling process.

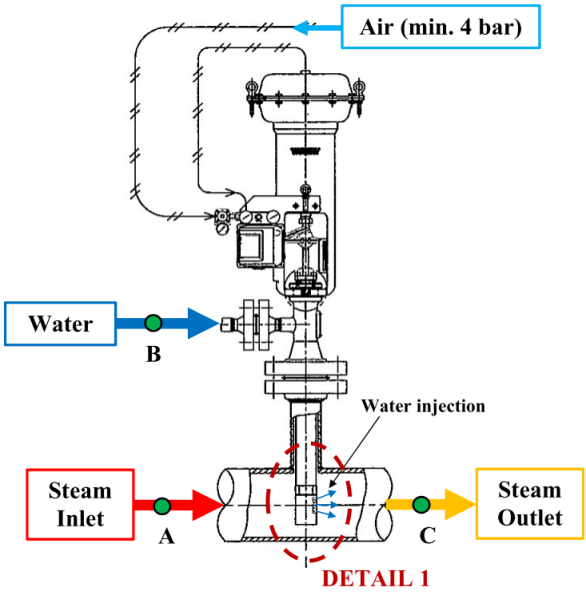

Figure 2 - Desuperheater and its operating fluids along with operating points (A, B and C) for the superheated steam cooling process thermodynamic analysis, reproduced from [31]

Detail 1 from Figure 2 is independently presented in Figure 3 with an aim to fully clarify Desuperheater cooling water injection principle. At the Desuperheater bottom on a long stem is mounted piston with piston rings which block cooling water

circulation through nozzles (in position as presented in Figure 3 where the cooling water injection did not occur). At the moment when cooling water should be injected into the superheated steam, Desuperheater pneumatic regulation moves stem downwards and the piston will open a cooling water channel to the first nozzle (Nozzle 1, Figure 3). At that position, cooling water will circulate between stem and Desuperheater housing and will be injected in superheated steam through the first nozzle. The shape of each nozzle ensures cooling water spray with water droplets as small as possible (smaller water droplets ensure better mixing with superheated steam).

At the moment when will be necessary to inject higher cooling water mass flow rate in superheated steam, Desuperheater pneumatic regulation system will move steam and piston more downwards in the housing and a channel to both first and second nozzles will be open (Nozzle 1 and Nozzle 2, Figure 3). In that situation cooling water will pass not through only one, but simultaneously through two nozzles. For the highest required cooling water mass flow rate, moving piston will be in the lowest possible position in the housing and in that situation cooling water will be injected through all three nozzles presented in Figure 3.

Reducing of injected cooling water mass flow rate will be performed by an opposite movement (Desuperheater regulation system will move stem and moving piston more and more upwards).

According to the producer specifications [32], the main aim of presented Desuperheater operation is to maintain wet steam (which will be delivered to auxiliary heaters) at approximately the same temperature in all power plant (steam system) operating regimes. This element can be ensured only by changing injected cooling water mass flow rate according to described procedure.

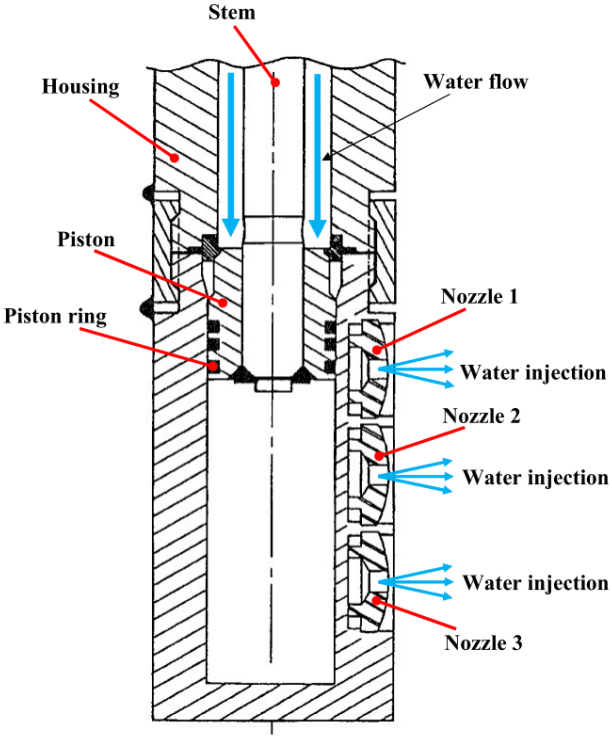

Figure 3 - Principle of cooling water injection into the superheated steam stream (Steam Inlet), Detail 1, reproduced from [32]

3. Equations for thermodynamic (energy and exergy) analysis of steam cooling process by using Desuperheater

Observation of steam cooling process and Desuperheater operation will be performed by using energy and exergy analyses. Energy analysis is based on the first law of thermodynamics and it did not consider the state of the ambient in which observed system, component or process operates [33, 34]. Exergy analysis is based on the second law of thermodynamics and it consider the ambient state [35, 36]. Therefore, it can be recommended that thermodynamic observation of any system, component or process should be performed by using both mentioned analyses, because the different kind of losses will be detected [37, 38]. Recently, in the observation of various systems, components and processes, exergy analysis found wider application in comparison to energy analysis and standard exergy analysis can be a baseline for further, much more complex analyses [39-41].

Both energy and exergy analyses have several basic equations and balances which should always be satisfied, regardless of the observed system, component or process specificity [42, 43]. The basic energy and exergy equations and balances can be found in the literature [44, 45]. The equations for the thermodynamic (energy and exergy) analysis of steam cooling process by using Desuperheater will be based on the mentioned basic equations and balances. Markings in all the equations presented in this section will be based on three operating points from Figure 2 (A, B and C). The observed steam cooling process is actually open cooling process (superheated steam and cooling water are mixed together), so the energy and exergy analyses can be performed as for any other open heater (for example, one of such open heater in steam power plants is Deaerator in which occurs steam and water mixing) [46, 47].

Main energy and exergy balance equations of the analyzed steam cooling process are [48, 49]:

$$\dot{E}n_{\mathrm{A}} + \dot{E}n_{\mathrm{B}} = \dot{E}n_{\mathrm{C}} + \dot{E}n_{\mathrm{LOSS}}\,, \tag{1}$$

$$\dot{E}x_{\mathrm{A}} + \dot{E}x_{\mathrm{B}} = \dot{E}x_{\mathrm{C}} + \dot{E}x_{\mathrm{LOSS}}\,, \tag{2}$$

where $\dot{E}n$ is a total energy and $\dot{E}x$ is a total exergy flow of each fluid stream (in each operating point). Total energy and exergy flows are defined by the following equations [50, 51]:

$$\dot{E}n = \dot{m}\cdot h\,, \tag{3}$$

$$\dot{E}x = \dot{m}\cdot \varepsilon\,. \tag{4}$$

In Eq. 3, is the operating medium specific enthalpy, while from Eq. 4 is operating medium specific exergy which definition can be found in [52, 53]:

$$\varepsilon = \left(h - h_0\right) - T_0\cdot\left(s - s_0\right). \tag{5}$$

In the energy and exergy balance equations of steam cooling process (Eq. 1 and Eq. 2), left equation parts represent energy (or exergy) input, while right equation parts represent the sum of energy (or exergy) output and losses. From the mentioned energy and exergy balance equations can be calculated energy and exergy losses of the observed steam cooling process:

$$\dot{E}n_{\mathrm{LOSS}} = \dot{E}n_{\mathrm{A}} + \dot{E}n_{\mathrm{B}} - \dot{E}n_{\mathrm{C}}\,, \tag{6}$$

$$\dot{E}x_{\mathrm{LOSS}} = \dot{E}x_{\mathrm{A}} + \dot{E}x_{\mathrm{B}} - \dot{E}x_{\mathrm{C}}\,. \tag{7}$$

Energy and exergy efficiency of the analyzed steam cooling process can be calculated by using equations:

$$\eta_{en} = \frac{\dot{E}n_C}{\dot{E}n_A + \dot{E}n_B} \tag{8}$$

$$\eta_{ex} = \frac{\dot{E}x_C}{\dot{E}x_A + \dot{E}x_B} \tag{9}$$

Mass flow rate balance for the observed steam cooling process is:

$$\dot{m}_A + \dot{m}_B = \dot{m}_C \,. \tag{10}$$

All presented equations are valid in each power plant operating regime. In the exergy analysis is essential to define the base ambient state for which the exergy analysis is performed. In this paper, the base ambient state is defined by the ambient temperature of 25 °C and the ambient pressure of 1 bar.

4. Measured parameters required for steam cooling process thermodynamic analysis

At each power plant (power system) load, required operating parameters for the energy and exergy analysis of the observed steam cooling process are temperature, pressure and mass flow rate of all fluids (in each operating point from Figure 2). These operating parameters are obtained by measurements during the marine steam power plant load increase. Steam operating parameters at the Desuperheater inlet and outlet (points A and C, Figure 2) are presented in Table 1, while cooling water operating parameters (point B, Figure 2) are presented in Table 2.

Table 1 - Operating parameters of steam at the Desuperheater Inlet and Outlet for various system loads

Load (%)*	Steam-Inlet (Operating Point A)**					Steam-Outlet (Operating Point C)**				
	Temp. (°C)	Pressure (bar)	Mass flow rate (kg/h)	Specific enthalpy (kJ/kg)	Specific exergy (kJ/kg)	Temp. (°C)	Pressure (bar)	Mass flow rate (kg/h)	Specific enthalpy (kJ/kg)	Specific exergy (kJ/kg)
0.00	200.91	10.79	2125	2825.80	845.49	183.09	10.76	2168	2763.80	823.09
2.52	244.84	10.77	3022	2928.70	886.21	183.04	10.75	3219	2753.80	819.49
7.03	238.56	10.85	2794	2914.20	881.08	183.33	10.82	2959	2750.00	819.00
13.47	230.30	10.83	2687	2895.40	873.08	183.29	10.81	2822	2752.00	819.57
32.49	219.88	10.79	2794	2871.40	862.96	183.04	10.75	2906	2761.80	822.26
26.14	222.31	10.79	2794	2877.10	865.22	183.09	10.76	2912	2759.80	821.70
35.58	221.64	10.84	2687	2875.30	865.11	183.33	10.82	2797	2752.00	819.70
35.34	225.32	10.81	2906	2884.00	868.22	183.17	10.78	3037	2747.90	817.79
38.14	223.77	10.81	2687	2880.40	866.78	183.21	10.79	2804	2755.90	820.70
41.71	222.75	10.88	2584	2877.70	866.55	183.37	10.83	2693	2750.00	819.13
43.33	225.09	10.74	2687	2883.80	867.29	182.88	10.71	2807	2765.60	823.13
47.05	226.73	10.76	2794	2887.50	869.03	182.88	10.71	2925	2769.70	824.52
48.22	227.49	10.84	2687	2888.90	870.56	183.29	10.81	2815	2754.00	820.26
49.79	228.20	10.80	2794	2890.70	870.81	183.09	10.76	2927	2751.80	818.92
51.47	228.36	10.84	2687	2890.90	871.37	183.21	10.79	2816	2755.90	820.70
52.08	227.91	10.74	2687	2890.30	869.91	182.88	10.71	2816	2765.60	823.13
57.65	226.29	10.82	2584	2886.20	869.23	183.25	10.80	2702	2770.00	825.69
61.97	222.89	10.82	2688	2878.30	866.06	183.17	10.78	2803	2761.90	822.65
66.99	222.83	10.79	2793	2878.30	865.70	183.04	10.75	2911	2755.80	820.18
73.77	223.38	10.85	2687	2879.30	866.82	183.33	10.82	2803	2766.00	824.56
75.17	224.19	10.74	2794	2881.70	866.45	182.84	10.70	2916	2757.60	820.23
77.74	222.23	10.75	2906	2877.10	864.74	182.92	10.72	3028	2763.70	822.57
79.25	350.41	11.03	1747	3157.00	998.02	183.86	10.95	2037	2766.50	826.23
83.22	350.01	11.30	3398	3155.60	1000.50	184.94	11.22	3962	2771.40	831.01
84.31	345.85	11.30	3268	3146.70	995.92	185.02	11.24	3856	2747.50	822.90

** Load is defined as a ratio of current and maximum main turbine power.*
*** According to operating points from Figure 2.*

Table 2 - Operating parameters of water at the Desuperheater Inlet for various system loads

Load (%)*	Water-Inlet (Operating Point B)**				
	Temperature (°C)	Pressure (bar)	Mass flow rate (kg/h)	Specific enthalpy (kJ/kg)	Specific exergy (kJ/kg)
0.00	134.65	30	43	568.03	71.46
2.52	131.39	30	197	554.16	67.77
7.03	131.31	30	165	553.79	67.67
13.47	131.40	30	135	554.18	67.77
32.49	131.00	30	112	552.48	67.33
26.14	131.45	30	118	554.39	67.83
35.58	129.92	30	110	547.89	66.13
35.34	129.97	30	131	548.09	66.18
38.14	129.71	30	117	546.98	65.89
41.71	129.80	30	109	547.39	66.00
43.33	129.79	30	120	547.36	65.99
47.05	129.58	30	131	546.46	65.75
48.22	128.89	30	128	543.51	64.99
49.79	127.56	30	133	537.87	63.54
51.47	127.57	30	129	537.89	63.55
52.08	126.76	30	129	534.48	62.67
57.65	125.90	30	118	530.79	61.74
61.97	125.99	30	115	531.21	61.85
66.99	126.76	30	118	534.47	62.67
73.77	126.84	30	116	534.78	62.75
75.17	126.68	30	122	534.12	62.58
77.74	127.86	30	122	539.15	63.87
79.25	126.86	30	290	534.89	62.78
83.22	127.84	30	564	539.03	63.84
84.31	127.94	30	588	539.48	63.95

** Load is defined as a ratio of current and maximum main turbine power.*
*** According to operating points from Figure 2.*

Steam and water specific enthalpies and specific entropies at each load are calculated from known pressure and temperature by using NIST-REFPROP 9.0 software [54], while steam and water specific exergies are calculated according to defined base ambient state by using Eq. 5.

All operating parameters in Table 1 and Table 2 are presented in relation to steam system load where the system load is defined as a ratio of current and maximum main turbine produced mechanical power. Therefore, it can be observed that the data are collected from the steam system startup (load of 0%) up to system load on which the specific fuel consumption is the lowest (load of 84.31%). Higher steam system loads were not achieved during measurements.

Measurements are performed by using standard measuring equipment already installed in the marine steam power plant. Each measuring device is calibrated, properly inspected and regularly maintained. In exploitation, mentioned measuring equipment is used for control and regulation purposes. The list of used measuring devices in each operating point from Figure 2 is presented in Table 3. All the details and full specifications related to each measuring device can be found on the producer website.

Table 3 - The list of used measuring equipment

Operating point*	Temperature	Pressure	Mass flow rate
A	Greisinger GTF 601-Pt100 - immersion probe [55]	Yamatake JTG940A - pressure transmitter [56]	Yamatake JTD960A - differential pressure transmitter [57]
B	Greisinger GTF 401-Pt100 - immersion probe [55]	Yamatake JTG960A - pressure transmitter [56]	Yamatake JTD960A - differential pressure transmitter [57]
C	Greisinger GTF 401-Pt100 - immersion probe [55]	Yamatake JTG940A - pressure transmitter [56]	Yamatake JTD960A - differential pressure transmitter [57]

** According to Figure 2.*

5. Results and discussion

As shown in Figure 4, for the observed steam cooling process can be concluded that superheated steam and cooling water mass flow rates follow each other at almost all observed steam system loads.

At three the highest steam system loads (79.25%, 83.22% and 84.31%) can be observed deviations from the above mentioned conclusion, but such deviations can be explained if (along with mass flow rates) are considered superheated steam and cooling water temperatures. According to Table 2, cooling water temperatures are very similar at each system load (around 130 °C), while the temperatures of superheated steam (at the Desuperheater inlet, Table 1) are notably higher at three the highest system loads (in comparison to lower system loads). Therefore, the decrease in superheated steam mass flow rate at load of 79.25% results with an increase in cooling water mass flow

rate, due to much higher superheated steam temperature in comparison to load of 77.74%. Increase in superheated steam mass flow rate between loads of 79.25% and 83.22% results also with an increase in cooling water mass flow rate. Between two the highest observed system loads (load of 83.22% and 84.31%) superheated steam mass flow rate and temperature decreases, while cooling water mass flow rate still slightly increases – what can be considered as a transient period after which cooling water mass flow rate will surely follow the mass flow rate of superheated steam.

Finally, it can be concluded that mass flow rates of cooling water and superheated steam in a properly balanced cooling process should have the same trends at different system loads. Any possible deviation from this conclusion can be expected only if a notable change in any fluid temperature occurs. Therefore, Desuperheater pneumatic regulation properly operates at all loads.

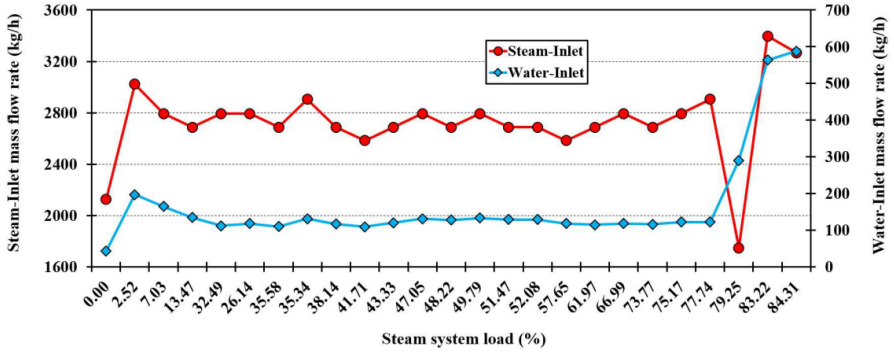

Figure 4 - Change in mass flow rate of water and superheated steam (at the Desuperheater inlet) during the steam system load increase

The main aim of Desuperheater operation is steam temperature reduction after water injection (at the Desuperheater outlet). Steam at the Desuperheater outlet is a wet steam (steam under the saturation line) with high steam content (between 97–99.5%, what depends on the current steam system load). Along with a reduction in temperature, at the Desuperheater outlet also occur reduction in steam pressure, Figure 5.

Steam at the Desuperheater outlet has slightly lower pressure in comparison to steam at the Desuperheater inlet, dominantly because of losses which occur during cooling and steam flow processes. Reduction in steam pressure is low and in the expected range for the analyzed process. It is interesting to note that a higher reduction in steam temperature also results with a higher reduction in steam pressure, what is clearly visible at the highest observed system loads, Figure 5.

Reduction in steam temperature is the lowest at the steam system startup, Figure 5. Temperature reduction transient field can be noted between steam system loads of 2.52% and 32.49%, after which reduction in steam temperature begins almost constant

(around 40 °C) during the increase in steam system load. Only at the highest observed loads, temperature reduction is notably higher in comparison to lower loads and equal to around 160 °C or more. The reason of such high temperature reduction at three the highest observed steam system loads (loads between 79.25% and 84.31%) can be found by observing steam temperatures in Table 1. The Desuperheater regulating system operates in a way that the steam temperature at the Desuperheater outlet remain always in a narrow range between 183 °C and 185 °C, regardless of steam system load. At three the highest steam system loads, steam temperature at the Desuperheater inlet is notably higher in comparison to lower loads (around 350 °C), so notably higher temperature reduction is required to remain approximately always the same steam temperature at the Desuperheater outlet. High steam temperature reduction at the highest observed loads is obtained by significantly higher cooling water mass flow rate injected into the superheated steam (in comparison to lower loads), Table 2.

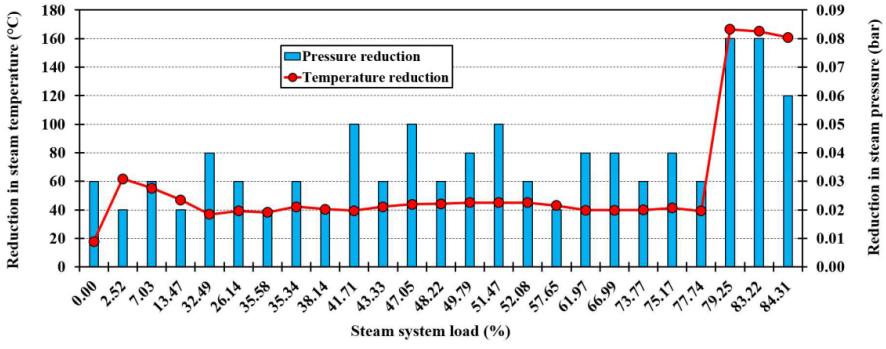

Figure 5 - Reduction of pressure and temperature at the Desuperheater outlet during the steam system load increase

Energy and exergy losses of the observed steam cooling process are low at almost all steam system loads (the exceptions can be seen at three the highest observed loads - 79.25%, 83.22% and 84.31%), Figure 6. Energy losses for all observed system loads are in range between 10–30 kW. At three the highest steam system loads energy loss did not exceed 15 kW, while at the highest system load of 84.31% energy loss is extremely small, almost negligible. Therefore, from the energy viewpoint can be concluded that steam cooling process has very low energy losses at all steam system loads (what can be usually expected for such kind of processes) and the lowest energy loss is obtained at the highest steam system load.

Exergy analysis shows different kind of losses in comparison to the energy analysis, therefore the conclusions obtained in energy analysis can strongly differ in regards to exergy analysis conclusions. Moreover, energy analysis of some systems or processes can be practically unusable due to its high dependence on the measurement

equipment accuracy and precision – one example can be found in [58] for a condensate/feedwater marine heating system.

Exergy analysis of the observed steam cooling process shows that the exergy losses are lower in comparison to energy losses (between 5–15 kW) for all system loads except three the highest ones (79.25%, 83.22% and 84.31%). At three the highest steam system loads can be observed, Figure 6, that exergy losses strongly increases and are higher than 20 kW (up to 40 kW). The reason of such high exergy losses at the highest system loads can be found in a fact that at mentioned loads in the steam is injected cooling water mass flow rate much higher in comparison to lower loads to ensure always approximately constant steam temperature at the Desuperheater outlet. As water has much lower specific exergies in comparison to steam (Table 1 and Table 2), increase in cooling water mass flow rate will result with increased exergy losses of the observed cooling system.

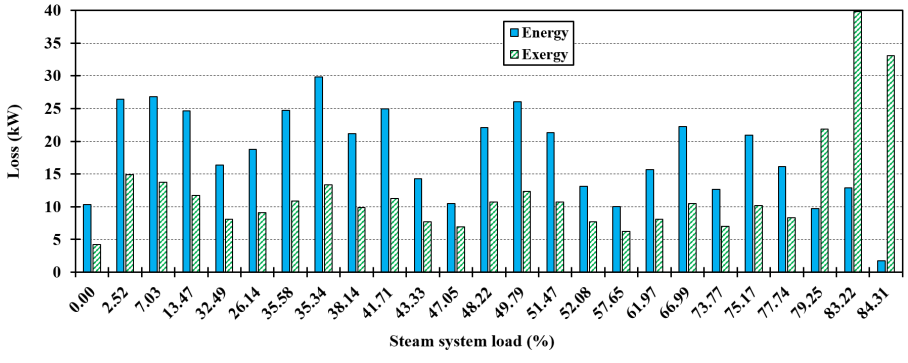

Figure 6 - Energy and exergy losses of superheated steam cooling process during the steam system load increase

The energy efficiency of a steam cooling process is very high (around 99% or higher) at all observed steam system loads, Figure 7. At the highest steam system load, efficiency of steam cooling process is almost perfect from the energy viewpoint (energy efficiency is very close to 100%), with almost negligible energy loss.

The exergy efficiency of the steam cooling process in all steam system loads (with an exception of three the highest loads) is slightly lower than energy efficiency, but still in the range of 98% or higher. At the highest steam system loads, due to a notable increase in cooling water mass flow rate and high temperature reduction, steam cooling process exergy efficiency significantly decreases, but still remains acceptably high (between 95% and 97%), Figure 7.

It should also be mentioned that trends in energy and exergy efficiency of steam cooling process are the same during the increase in steam system load, Figure 7. The same similarity in energy and exergy trends during the increase in steam system load

can be seen for losses, Figure 6. Slight deviations can be seen only at three the highest steam system loads (79.25%, 83.22% and 84.31%).

Observing both energy and exergy losses and efficiencies (Figure 6 and Figure 7) it can be concluded that exergy analysis consider notable increase in mass flow rate of fluid (water) which thermodynamic properties strongly differs in comparison to steam (regardless if the steam is superheated or wet). Such element cannot be seen in the energy analysis of the same system. Therefore, it is advisable to use both energy and exergy analyses in the observation of any system or a component.

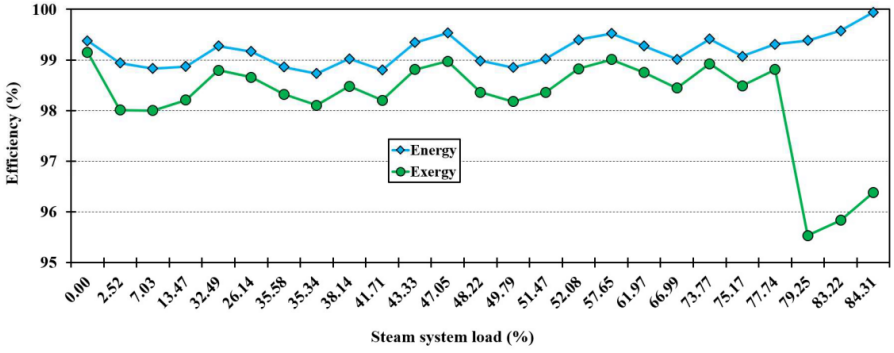

Figure 7 - Energy and exergy efficiencies of superheated steam cooling process during the steam system load increase

Further research related to the observed system and its influence on the overall marine power plant performance will be performed by using various complex artificial intelligence methods and processes [59-61].

6. Conclusions

In this paper is performed thermodynamic (energy and exergy) analysis of the steam cooling process in the marine steam propulsion plant by using Desuperheater. Desuperheater is pneumatically regulated device which inject cooling water in the superheated steam with an aim to obtain wet steam. Wet steam at the Desuperheater outlet is used in auxiliary heaters for various heating purposes onboard LNG carrier. Auxiliary heaters require wet steam for its operation due to safety reasons and for easier steam condensation after all heating purposes are satisfied. It is investigated how the change in dominant operating parameters of all fluids influences steam cooling process, its losses and efficiencies for a variety of marine steam system loads. In the performed analysis are used operating parameters measured in the steam system during exploitation. The most important conclusions of the performed analysis are:

- Mass flow rates of cooling water and superheated steam in a properly balanced cooling process should have the same trends at different system loads. Any deviations from this conclusion can be explained if superheated steam and cooling water temperatures are considered, along with mass flow rates.
- Steam at the Desuperheater outlet is a wet steam (steam under the saturation line) with high steam content (between 97–99.5%). The exact steam content depends on the current steam system load.
- Steam at the Desuperheater outlet has slightly lower pressure in comparison to steam at the Desuperheater inlet, dominantly because of losses which occur during cooling and steam flow processes. Reduction in steam pressure is low and in the expected range for such process. Also, a higher reduction in steam temperature simultaneously results with a higher reduction in steam pressure.
- Reduction in steam temperature is the lowest at the steam system startup. During the most observed steam system loads, reduction in steam temperature is almost constant (around 40 °C). Only at the highest observed loads, temperature reduction is notably higher and equal to around 160 °C or more. Reduction in steam temperature is dependable on the superheated steam temperature (Desuperheater inlet) because the temperature of wet steam (Desuperheater outlet) is intended to be almost constant at all steam system loads.
- Energy losses of steam cooling process for all observed system loads are in range between 10–30 kW. At three the highest steam system loads energy loss did not exceed 15 kW, while at the highest load energy loss is almost negligible.
- Exergy losses of the same system are lower in comparison to energy losses (between 5–15 kW) for all system loads except three the highest ones. At three the highest loads exergy losses strongly increase and are higher than 20 kW (up to 40 kW). The reason of such occurrence is found in a fact that at the highest loads in the superheated steam is injected cooling water mass flow rate much higher in comparison to lower loads.
- Energy efficiency of a steam cooling process is very high (around 99% or higher) at all observed steam system loads. The exergy efficiency of the steam cooling process in all steam system loads (with an exception of three the highest loads) is slightly lower than energy efficiency, but still in the range of 98% or higher. At the highest steam system loads, due to a notable increase in cooling water mass flow rate and high temperature reduction, steam cooling process exergy efficiency significantly decreases, but still remains acceptably high (between 95% and 97%).
- Trends in energy and exergy efficiency of steam cooling process are the same during the increase in steam system load. The same is valid for energy and exergy loss of the steam cooling process during the increase in steam system load.
- Observation of both energy and exergy losses and efficiencies leads to conclusion that exergy analysis consider notable increase in mass flow rate of cooling water, which thermodynamic properties (especially specific exergies) strongly differs in comparison to steam. Such element cannot be seen in the energy analysis of the same system.

Acknowledgment

This research has been supported by the Croatian Science Foundation under the project IP-2018-01-3739 and University of Rijeka scientific grants: uniri-tehnic-18-18-1146 and uniri-tehnic-18-14.

NOMENCLATURE

Abbreviations

DWT	Dead Weight Tonnage
HPC	High Pressure Cylinder
LNG	Liquefied Natural Gas
LPC	Low Pressure Cylinder
SG	Steam Generator
TG	Turbo-Generator

Latin symbols

$\dot{E}n$	total energy flow, kW
$\dot{E}x$	total exergy flow, kW
h	specific enthalpy, kJ/kg
$\dot{m}$	mass flow rate, kg/h
p	pressure, bar
s	specific entropy, kJ/kg·K
T	temperature, K or °C

Greek symbols

ε	specific exergy, kJ/kg
η	efficiency, %

Subscripts

0	base ambient state
en	energy
ex	exergy

References

1. Tadros, M., Ventura, M., & Soares, C. G. (2019). Optimization procedure to minimize fuel consumption of a four-stroke marine turbocharged diesel engine. *Energy*, 168, 897-908. (doi:10.1016/j.energy.2018.11.146)
2. Altosole, M., Campora, U., Figari, M., Laviola, M., & Martelli, M. (2019). A diesel engine modelling approach for ship propulsion real-time simulators. *Journal of Marine Science and Engineering*, 7(5), 138. (doi:10.3390/jmse7050138)
3. Senčić, T., Mrzljak, V., Medica-Viola, V., & Wolf, I. (2022). CFD Analysis of a Large Marine

Engine Scavenging Process. *Processes*, 10(1), 141. (doi:10.3390/pr10010141)
4. Muše, A., Jurić, Z., Račić, N., & Radica, G. (2020). Modelling, performance improvement and emission reduction of large two-stroke diesel engine using multi-zone combustion model. *Journal of Thermal Analysis and Calorimetry*, 141(1), 337-350. (doi:10.1007/s10973-020-09321-7)
5. Ma, C., Yao, C., Song, E. Z., & Ding, S. L. (2021). Prediction and optimization of dual-fuel marine engine emissions and performance using combined ANN with PSO algorithms. *International Journal of Engine Research*, 1468087421990476. (doi:10.1177/1468087421990476)
6. Pham, V. C., Rho, B. S., Kim, J. S., Lee, W. J., & Choi, J. H. (2021). Effects of various fuels on combustion and emission characteristics of a four-stroke dual-fuel marine engine. *Journal of Marine Science and Engineering*, 9(10), 1072. (doi:10.3390/jmse9101072)
7. Liu, L., Wu, Y., & Wang, Y. (2022). Numerical investigation on knock characteristics and mechanism of large-bore natural gas dual-fuel marine engine. *Fuel*, 310, 122298. (doi:10.1016/j.fuel.2021.122298)
8. Lamas Galdo, M. I., Castro-Santos, L., & Rodriguez Vidal, C. G. (2020). Numerical analysis of NOx reduction using ammonia injection and comparison with water injection. *Journal of Marine Science and Engineering*, 8(2), 109. (doi:10.3390/jmse8020109)
9. Senčić, T., Mrzljak, V., Blecich, P., & Bonefačić, I. (2019). 2D CFD simulation of water injection strategies in a large marine engine. *Journal of Marine Science and Engineering*, 7(9), 296. (doi:10.3390/jmse7090296)
10. Kozina, A., Radica, G., & Nižetić, S. (2020). Analysis of methods towards reduction of harmful pollutants from diesel engines. *Journal of Cleaner Production*, 262, 121105. (doi:10.1016/j.jclepro.2020.121105)
11. Bai, M., Liu, J., Ma, Y., Zhao, X., Long, Z., & Yu, D. (2021). Long short-term memory network-based normal pattern group for fault detection of three-shaft marine gas turbine. *Energies*, 14(1), 13. (doi:10.3390/en14010013)
12. Anđelić, N., Mrzljak, V., Lorencin, I., & Baressi Šegota, S. (2020). Comparison of Exergy and Various Energy Analysis Methods for a Main Marine Steam Turbine at Different Loads. *Pomorski zbornik*, 59(1), 9-34. (doi:10.18048/2020.59.01)
13. Koroglu, T., & Sogut, O. S. (2018). Conventional and advanced exergy analyses of a marine steam power plant. *Energy*, 163, 392-403. (doi:10.1016/j.energy.2018.08.119)
14. Huan, T., Hongjun, F., Wei, L., & Guoqiang, Z. (2019). Options and evaluations on propulsion systems of LNG carriers. In *Propulsion systems* (pp. 1-20). London, UK: IntechOpen.
15. Anđelić, N., Baressi Šegota, S., Lorencin, I., Poljak, I., Mrzljak, V., & Car, Z. (2021). Use of Genetic Programming for the Estimation of CODLAG Propulsion System Parameters. *Journal of Marine Science and Engineering*, 9(6), 612. (doi:10.3390/jmse9060612)
16. Fernández, I. A., Gómez, M. R., Gómez, J. R., & Insua, Á. B. (2017). Review of propulsion systems on LNG carriers. *Renewable and Sustainable Energy Reviews*, 67, 1395-1411. (doi:10.1016/j.rser.2016.09.095)
17. George, D. G., Eleftherios, K. D., & Chariklia, G. A. (2020). LNG carrier two-stroke propulsion systems: A comparative study of state of the art reliquefaction technologies. *Energy*, 195, 116997. (doi:10.1016/j.energy.2020.116997)
18. Ammar, N. R. (2019). Environmental and cost-effectiveness comparison of dual fuel propulsion options for emissions reduction onboard LNG carriers. *Brodogradnja: Teorija i praksa brodogradnje i pomorske tehnike*, 70(3), 61-77. (doi:10.21278/brod70304)
19. Çiçek, A. N. (2009). Exergy analysis of a crude oil carrier steam plant (Doctoral dissertation, Istanbul Technical University).
20. Lorencin, I., Anđelić, N., Mrzljak, V., & Car, Z. (2019). Multilayer perceptron approach to condition-based maintenance of marine CODLAG propulsion system components. *Pomorstvo*, 33(2), 181-190. (doi:10.31217/p.33.2.8)
21. Emhofer, J., Marx, K., Sporr, A., Barz, T., Nitsch, B., Wiesflecker, M., & Pink, W. (2022). Experimental demonstration of an air-source heat pump application using an integrated phase change material storage as a desuperheater for domestic hot water generation. *Applied Energy*, 305, 117890. (doi:10.1016/j.apenergy.2021.117890)
22. Liang, H., Zhao, B., Huang, C., Song, H., & Jiang, X. (2021). Numerical simulation study on performance optimization of desuperheater. *Energy Reports*, 7, 2221-2232. (doi:10.1016/j.egyr.2021.04.023)

23. Main boilers operation and maintenance instructions (MB-4E-KS), Mitsubishi Heavy Industries Ltd, Nagasaki Shipyard & Machinery Works, Nagasaki, Japan, 2005. (internal ship documentation)
24. Mrzljak, V., Poljak, I., & Medica-Viola, V. (2017). Dual fuel consumption and efficiency of marine steam generators for the propulsion of LNG carrier. *Applied Thermal Engineering*, 119, 331-346. (doi:10.1016/j.applthermaleng.2017.03.078)
25. Mrzljak, V., Prpić-Oršić, J., & Senčić, T. (2018). Change in steam generators main and auxiliary energy flow streams during the load increase of LNG carrier steam propulsion system. *Pomorstvo*, 32(1), 121-131. (doi:10.31217/p.32.1.15)
26. Mrzljak, V., Poljak, I., & Mrakovčić, T. (2017). Energy and exergy analysis of the turbo-generators and steam turbine for the main feed water pump drive on LNG carrier. *Energy conversion and management*, 140, 307-323. (doi:10.1016/j.enconman.2017.03.007)
27. Mrzljak, V., Poljak, I., & Prpić-Oršić, J. (2019). Exergy analysis of the main propulsion steam turbine from marine propulsion plant. *Brodogradnja: Teorija i praksa brodogradnje i pomorske tehnike*, 70(1), 59-77. (doi:10.21278/brod70105)
28. Mrzljak, V., Poljak, I., & Medica-Viola, V. (2016). Efficiency and losses analysis of low-pressure feed water heater in steam propulsion system during ship maneuvering period. *Pomorstvo*, 30(2), 133-140. (doi:10.31217/p.30.2.6)
29. Mrzljak, V., Poljak, I., & Medica-Viola, V. (2017). Thermodynamical analysis of high-pressure feed water heater in steam propulsion system during exploitation. *Brodogradnja: Teorija i praksa brodogradnje i pomorske tehnike*, 68(2), 45-61. (doi:10.21278/brod68204)
30. Poljak, I., Bielić, T., Mrzljak, V., & Orović, J. (2020). Analysis and Optimization of Atmospheric Drain Tank of Lng Carrier Steam Power Plant. *Journal of Marine Science and Engineering*, 8(8), 568. (doi:10.3390/jmse8080568)
31. Yarway TempLow Desuperheater, Specification & Drawing, Hyundai Heavy Industries Co., Tyco Flow Control K. K., Kobe - Tokyo, Japan, 2006. (internal ship documentation)
32. Installation, operation and maintenance of the TempLow steam desuperheater, Yarway Co., Tyco Flow Control, Kobe, 1993. (internal ship documentation)
33. Gospić, I., Glavan, I., Poljak, I., & Mrzljak, V. (2021). Energy, Economic and Environmental Effects of the Marine Diesel Engine Trigeneration Energy Systems. *Journal of Marine Science and Engineering*, 9(7), 773. (doi:10.3390/jmse9070773)
34. Kanoğlu, M., Çengel, Y. A., & Dinçer, İ. (2012). Efficiency evaluation of energy systems. Springer Science & Business Media.
35. Dincer, I., & Rosen, M. A. (2012). Exergy: energy, environment and sustainable development. Newnes.
36. Szargut, J. (2005). Exergy method: technical and ecological applications (Vol. 18). WIT press.
37. Baldi, F., Ahlgren, F., Nguyen, T. V., Thern, M., & Andersson, K. (2018). Energy and exergy analysis of a cruise ship. *Energies*, 11(10), 2508. (doi:10.3390/en11102508)
38. Ogorure, O. J., Oko, C. O. C., Diemuodeke, E. O., & Owebor, K. (2018). Energy, exergy, environmental and economic analysis of an agricultural waste-to-energy integrated multigeneration thermal power plant. *Energy conversion and management*, 171, 222-240. (doi:10.1016/j.enconman.2018.05.093)
39. Nasruddin, N., Saputra, I. D., Mentari, T., Bardow, A., Marcelina, O., & Berlin, S. (2020). Exergy, exergoeconomic, and exergoenvironmental optimization of the geothermal binary cycle power plant at Ampallas, West Sulawesi, Indonesia. *Thermal Science and Engineering Progress*, 19, 100625. (doi:10.1016/j.tsep.2020.100625)
40. Nourpour, M., Khoshgoftar Manesh, M. H., Pirozfar, A., & Delpisheh, M. (2021). Exergy, Exergoeconomic, Exergoenvironmental, Emergy-based Assessment and Advanced Exergy-based Analysis of an Integrated Solar Combined Cycle Power Plant. *Energy & Environment*, 0958305X211063558. (doi:10.1177/0958305X211063558)
41. Wang, J., Lu, Z., Li, M., Lior, N., & Li, W. (2019). Energy, exergy, exergoeconomic and environmental (4E) analysis of a distributed generation solar-assisted CCHP (combined cooling, heating and power) gas turbine system. *Energy*, 175, 1246-1258. (doi:10.1016/j.energy.2019.03.147)
42. Medica-Viola, V., Baressi Šegota, S., Mrzljak, V., & Štifanić, D. (2020). Comparison of conventional and heat balance based energy analyses of steam turbine. *Pomorstvo*, 34(1), 74-85. (doi:10.31217/p.34.1.9)

43. Mrzljak, V., Anđelić, N., Lorencin, I., & Sandi Baressi Šegota, S. (2021). The influence of various optimization algorithms on nuclear power plant steam turbine exergy efficiency and destruction. *Pomorstvo*, 35(1), 69-86. (doi:10.31217/p.35.1.8)
44. Ahmadi, G. R., & Toghraie, D. (2016). Energy and exergy analysis of Montazeri steam power plant in Iran. *Renewable and Sustainable Energy Reviews*, 56, 454-463. (doi:10.1016/j.rser.2015.11.074)
45. Adibhatla, S., & Kaushik, S. C. (2014). Energy and exergy analysis of a super critical thermal power plant at various load conditions under constant and pure sliding pressure operation. *Applied thermal engineering*, 73(1), 51-65. (doi:10.1016/j.applthermaleng.2014.07.030)
46. Eke, M. N., Onyejekwe, D. C., Iloeje, O. C., Ezekwe, C. I., & Akpan, P. U. (2018). Energy and exergy evaluation of a 220MW thermal power plant. *Nigerian Journal of Technology*, 37(1), 115-123. (doi:10.4314/njt.v37i1.15)
47. Noroozian, A., Mohammadi, A., Bidi, M., & Ahmadi, M. H. (2017). Energy, exergy and economic analyses of a novel system to recover waste heat and water in steam power plants. *Energy conversion and management*, 144, 351-360. (doi:10.1016/j.enconman.2017.04.067)
48. Khaleel, O. J., Ibrahim, T. K., Ismail, F. B., & Al-Sammarraie, A. T. (2021). Developing an analytical model to predict the energy and exergy based performances of a coal-fired thermal power plant. *Case Studies in Thermal Engineering*, 28, 101519. (doi:10.1016/j.csite.2021.101519)
49. Mrzljak, V., Kudláček, J., Baressi Šegota, S., & Medica-Viola, V. (2021). Energy and Exergy Analysis of Waste Heat Recovery Closed-Cycle Gas Turbine System while Operating with Different Medium. *Pomorski zbornik*, 60(1), 21-48. (doi:10.18048/2021.60.02)
50. Erdem, H. H., Akkaya, A. V., Cetin, B., Dagdas, A., Sevilgen, S. H., Sahin, B., ... & Atas, S. (2009). Comparative energetic and exergetic performance analyses for coal-fired thermal power plants in Turkey. *International Journal of Thermal Sciences*, 48(11), 2179-2186. (doi:10.1016/j.ijthermalsci.2009.03.007)
51. Mrzljak, V., Prpić-Oršić, J., & Poljak, I. (2018). Energy power losses and efficiency of low power steam turbine for the main feed water pump drive in the marine steam propulsion system. *Pomorski zbornik*, 54(1), 37-51. (doi:10.18048/2018.54.03)
52. Aljundi, I. H. (2009). Energy and exergy analysis of a steam power plant in Jordan. *Applied thermal engineering*, 29(2-3), 324-328. (doi:10.1016/j.applthermaleng.2008.02.029)
53. Tan, H., Shan, S., Nie, Y., & Zhao, Q. (2018). A new boil-off gas re-liquefaction system for LNG carriers based on dual mixed refrigerant cycle. *Cryogenics*, 92, 84-92. (doi:10.1016/j.cryogenics.2018.04.009)
54. Lemmon, E. W., Huber, M. L., & McLinden, M. O. (2010). NIST Standard Reference Database 23, Reference Fluid Thermodynamic and Transport Properties (REFPROP), version 9.0, National Institute of Standards and Technology. R1234yf. fld file dated December, 22, 2010.
55. https://www.greisinger.de/files/upload/en/produkte/kat/k16_011_EN_oP.pdf (accessed: 10.02.2022.)
56. https://www.datasheetarchive.com (accessed: 10.02.2022.)
57. https://www.ontrium.com/get.aspx?id=890511 (accessed: 10.02.2022.)
58. Mrzljak, V., Lorencin, I., Anđelić, N., & Car, Z. (2021). Thermodynamic Analysis of a Condensate Heating System from a Marine Steam Propulsion Plant with Steam Reheating. *Journal of Marine Science and Application*, 20(1), 117-127. (doi:10.1007/s11804-021-00191-5)
59. Baressi Šegota, S., Lorencin, I., Musulin, J., Štifanić, D., & Car, Z. (2020). Frigate speed estimation using CODLAG propulsion system parameters and multilayer perceptron. *NAŠE MORE: znanstveni* časopis *za more i pomorstvo*, 67(2), 117-125. (doi:10.17818/NM/2020/2.4)
60. Lorencin, I., Anđelić, N., Mrzljak, V., & Car, Z. (2019). Genetic algorithm approach to design of multi-layer perceptron for combined cycle power plant electrical power output estimation. *Energies*, 12(22), 4352. (doi:10.3390/en12224352)
61. Baressi Šegota, S., Lorencin, I., Ohkura, K., & Car, Z. (2019). On the traveling salesman problem in nautical environments: an evolutionary computing approach to optimization of tourist route paths in Medulin, Croatia. *Pomorski zbornik*, 57(1), 71-87. (doi:10.18048/2019.57.05)